KFKI-1981-62

Z.GY. HORVÁTH
S. VARRÓ

FRESNEL REFLEXION HALO LASERS

Hungarian Academy of Sciences

CENTRAL
RESEARCH
INSTITUTE FOR
PHYSICS

BUDAPEST

2017

KFKI-1981-62

FRESNEL REFLEXION HALO LASERS

Z.Gy. Horváth and S. Varró

Central Research Institute for Physics
H-1525 Budapest 114, P.O.B. 49, Hungary

HU ISSN 0368 5330
ISBN 963 371 844 9

ABSTRACT

Planar laser action of two-dimensional disc-shaped active material is reviewed for the light emerging because of Fresnel reflexions in the partly closed cylindrical Fabry-Perot resonator constituting the natural surrounding of the material. The calculations presented show that a proper choice of pumping permits the value and the spatial distribution of the gain to be conveniently set. This enable us obtaining a single mode planar laser.

АННОТАЦИЯ

Рассмотрен принцип действия двумерного плоскостного лазера с дискообразным активным материалом,в котором генерация возникает на френелевских отражениях,возникающих на поверхности активного материала, создающего отчасти замкнутый цилиндрический резонатор Фабри-Перо. Описанные расчеты показывают, что при соответствующем подборе величины и пространственного распределения накачки дается достичь режим одномодовой генерации в двумерном плоскостном лазере.

KIVONAT

A siklézer müködést tekintjük át kétdimenziós, tárcsa alaku aktiv anyagokban, melyekben a lézermüködés azon Fresnel reflexiók miatt alakul ki,melyek a lézeranyag természetes határfelületén lépnek fel, és részben zárt, henger alaku Fabry-Perot rezonátort alkotnak. Az itt közölt számitások azt mutatják, hogy a gerjesztés értékének és térbeli eloszlásának célszerü megválasztásával lehetőség nyilik egymódusu siklézer megvalósitására.

I. INTRODUCTION

It has recently been shown [1], [2] that linear one-dimensional laser operation is not an inherent consequence of laser physical processes but that it is due to the line-like formation of lasers stemming from the use of an open Fabry-Perot resonator, i.e. the conventional construction of laser devices.

As experimental evidence of this statement, a two-dimensional, planar, so-called halo superradiance [3], [4] then a true halo laser were produced in a partly closed two-dimensional Fabry-Perot resonator [1], [2]. The distinct denomination is justified by the fact that this halo phenomenon essentially differs from the so-called planar laser obtained by Nicoll [5] and from the known two-dimensional DFB lasers [6], [7].

Sources of amplified spontaneous emissions (ASE) generating disc-shaped or spherical radiation have long since been the subject of theoretical studies in connection with light amplification processes in astrophysics [8]. Most recently Hardy and Treves [9] have analysed the possibilities of ASE in disc-shaped or spherical dye lasers. Our experiments have shown the extreme difficulties of observing ASE in disc-shaped two-dimensional laser material because of the halo laser process previously initiated by reflexions from the natural surface boundary of systems with a high amplification factor [2]. In the case of low excitation, fluorescence can be observed; then, as the pumping rate is gradually increased, first the light scattered on the defects of the material is seen to emerge from the "whispering" modes imprisoned because of total reflexion, then the eventually "shouting" modes capable of emerging are emitted in the form of a true halo laser.

The ASE described in [9] can be observed if, for example the Fresnel reflexions from the natural boundaries of the active material are negligible. This can happen in cosmic space where the material density gradient is almost zero over a wide region of the boundary. Similarly, a superradiance becomes possible if the two-dimensional laser process takes place in a time short enough (a few picoseconds) to prevent the light from reaching the reflecting boundary surfaces [3], [4].

The purpose of the present work is to review the experimentally easily verifiable processes which are initiated in halo lasers by inevitable Fresnel

reflexions from the natural boundary of the disc-shaped active material. We will henceforth call these lasers "Fresnel Reflexion Halo Lasers". Radiations fromed by using artifical (e.g. dielectric) mirrors, or DFB obtainable in the form of concentric circles of gain or density of the active material are not included in this review.

The disturbing properties of "whispering" modes have already been studied by several workers, particularly, in the case of disc-shaped amplifiers [10], [11]. In the present study of halo lasers it is the "shouting" modes which are of interest, thus the analysis is restricted to the latter. (It should be noted that judging by experimental evidence, the "whispering" modes play an important part as energy stores in connection with a phenomenon not observed in one-dimensional lasers, namely, in that the duration of halo laser pulses considerably increases as compared with the picosecond duration of the excitation [3], [4].)

Similarly to conventional lasers, the production of standing waves is required also for the initiation of true two-dimensional laser processes. For this reason the possible halo laser modes are searched for in the form of light pahts running along closed polygons which are generated in cylindrical, partly closed, two-dimensional Fabry-Perot resonator - similarly to the case of ring lasers. However, there is an essential difference from the latter principle: the light paths associated in the ring lasers with the polygon are localized due to the position of mirrors whereas the light paths which form at any point of the cylindrical resonator are collective in the halo laser of rotational symmetry.

Cylindrical resonators are well-known and have long been used in microwave techniques. The same principle has to be generalized and extended in the same way as was done in one of the most important steps in the development of one-dimensional lasers [12]. In principle, we are again faced with the problem of determining the operational conditions of a resonator with dimensions which must substantially exceed the wavelength of the laser.

Phenomena taking place in halo lasers are investigated, above all, in order to see how to obtain a planar halo laser operating in a single mode and how to select this mode in the case of Fresnel reflexions from the numerous possible modes by modifying the spatial distribution and the value of pumping. The analysis is intended to prove that a substantial reduction of modes can be achieved not only in one dimensional open Fabry-Perot resonators. Incidentally, it was precisely the possible suppression of modes for which the open resonators were originally adopted in the design of laser devices [12].

For simplicity, the competition between modes is nowhere taken into account in the calculations, consequently, the results offered provide a good qualitative picture of the essential processes taking place in halo lasers. The calculations reveal phenomena which radically differ from those observed up to now in one-dimensional lasers. It can be expected that by refining the procedures further special laser physical processes will be revealed which

could offer a wide possibility for the use of two- or three-dimensional monochromatic laser lamps both in research and application.

Assuming light paths along different chords of a circle, we will first analyse the conditions of gain and the emergence of ASE or superradiance for homogeneous pumping: then, for pumping of circular symmetry with Gaussian type distribution postulating the use of active material with a cylindrical boundary surface. Subsequently, the formation of possible closed polygonal modes and the conditions of two-dimensional laser operation will be considered in double-walled resonators which more precisely reproduce the experimental conditions for dye halo lasers.

The effect of annular excitation on mode selection as well as the special properties of the divergence normal to the operational plane of the halo laser are dealt with in separate sections. Finally the values of the free spectral range (FSR) needed for the spectral identification of modes and phenomena observed during the spatial separation of planar laser modes emerging from the halo laser are discussed.

The description holds for the steady state and concrete laser materials but the actual type of excitation is not dealt with.

II. HOMOGENEOUS EXCITATION

Planar lasers with a radiation different from superradiance require the use of a two-dimensional resonator to secure feedback. The most convenient is to surround disc-shaped laser material with a partly closed two-dimensional Fabry-Perot resonator, actually, a reflector of cylindrical surface.

We restrict ourselves, in this paper, to phenomena taking place when the active material is "left alone", that is, when no reflector is being used. In this case the boundary between the laser material and air or vacuum and that between the laser material and the container wall act as the resonator of the two-dimensional laser because natural reflexions occur due to a change in the value of the refraction index on the natural interfaces. The measure of natural reflexions is unequivocally determined by Fresnel's equations. Lasers are thus called Fresnel Reflexion Halo Lasers if the boundary surface of the active material acts as a reflector.

First, we have to determine the intensity of the light emitted in the radiation observed along a chord of the circular active material.

For simplicity, some restrictions are made. The laser material is taken to be planar, of circular form with radius R, and of negligible thickness. Thus, the divergence normal to the plane will be neglected. Later (in Section VI) an estimate will be given on the extent of divergence. The circular planar source is homogeneously pumped from a direction normal to its plane. Consequently, the excitation has the same value at any point of the circle. This implies that in our calculation the coefficient of the exponential gain is taken to be constant in space and time expect for the case of Gaussian excitation. Competition between modes will also be omitted thus the operation of individual modes will not affect the value of g.

Symbols used in our calculation are specified in the insert of Fig. 1. The chosen light path lies at angle α to the diameter and the intensity of the emitted light is evaluated as a function of α at different gain values. Let us suppose that starting from the wall a ray of light with intensity I_o and at angle α to the diameter reaches the point of first reflexion.

Each further reflexion of this ray of light is still at angle α to the diameter, i.e. to the radius drawn to the point of reflexion.

The measure of reflexion can now be evaluated by use of Fresnel's formulae.

The reflexion coefficient for light polarized in a parallel direction with the plane of radiation is given as

$$\rho_{\parallel}(\alpha) = \left(\frac{n - \frac{\cos\delta}{\cos\alpha}}{n + \frac{\cos\delta}{\cos\alpha}} \right)^2 \qquad (1)$$

that for light polarized in a direction normal to that plane is

$$\rho_{\perp}(\alpha) = \left(\frac{\frac{n\cos\delta}{\cos\alpha} - 1}{\frac{n\cos\delta}{\cos\alpha} + 1} \right)^2 , \qquad (2)$$

where

$$\delta = \arcsin\left(\frac{\sin\alpha}{n}\right) ,$$

and $n = \frac{n_o}{n_1}$ is the relative refraction coefficient where n_1 and n_o are the coefficients of the active material and of the environment, respectively.

The next point of reflexion is reached by the above ray of light over a path of length

$$\ell(\alpha) = 2R\cos\alpha .$$

It follows from the above that the light which started at intensity I_o, after k reflexions is emitted from the cuvette with an intensity

$$I_k(\alpha) = I_o \rho(\alpha)^{k-1} e^{2Rpg_o k\cos\alpha}(1-\rho(\alpha)) , \qquad (3)$$

where the term $(1-\rho(\alpha))$ describes the transmission.

The pumping parameter p is expressed as

$$p = \frac{g}{g_o}$$

by which the current actual value of the gain is related to that of the threshold gain. In this way parameter p is independent of R.

According to definition, the threshold gain is g_o if the light emerges after having covered the diagonal path to and from with intensity I_o. This means that the total internal net gain is equal to unity and that it can be expressed as

$$\rho(0)e^{4Rg_o} = 1 \quad ,$$

hence

$$g_o = -\frac{\ln\rho(0)}{4R} \quad . \tag{4}$$

If R and n are given, g_o can unambiguously be evaluated since the values of $\rho(0)$ are the same for both polarizations in the case of normal incidence:

$$\rho_\perp(0) = \rho_\parallel(0) = \left(\frac{n-1}{n+1}\right)^2 \quad .$$

In Figs. 1. and 2. the variations of the value of $\frac{I(\alpha)}{I_o}$ with the angle to the diagonal are plotted for both directions of polarization, at different values of p. Numerical values were chosen to be: R = 1, n_o = 1, n_1 = 1.51, n = 0.66, k = 2, g_o = 0.8.

Solid lines in the figures show the range in which the net internal gain (without transmission multiplicator) amounts to unity.

It is of interest to note that for threshold excitation (p = 1) the intensity of the light of polarization in the direction parallel to the plane does not reach the threshold except for the diagonal (by which the threshold gain is actually defined) and that below the threshold value it is close to the value it would reach at the angle of total reflexion. Another phenomenon of interest is that because of the high value of the reflexion coefficient the intensity of polarization normal to the operational plane exceeds the threshold gain even for a pumping parameter p = 0.2 though only a fraction of the internal light is capable of emergence in the range near to the total reflexion. This fact is of great importance in the halo laser by total internal reflexion behave as energy stores from which the energy can be pumped (for a time determined by the lifetime of fluorescence) into modes capable of emergence. This is why the halo laser excited by picosecond pulses was observed to operate for a time exceeding by three orders of magnitude that of the excitation, a phenomenon never observed in one-dimensional devices [3].

The pictures reproduced in Figs 1. and 2. are good illustrations even for twofold reflexion (k = 2) of the actual process which, in fact, is only quantitatively influenced by the number of reflexions. The numerical value of the intensity depends on the powers of the overall internal net gain. It is only the lower or higher value of the net gain relative to unity which is decisive for laser operation. The actual operation is enhanced but not changed by the power dependence. For a given gain the operation is thus determined by the overall gain along a chord and by the associated reflexions.

The polarization of the emerging light is determined by the degree of polarization estimated from the different intensities of light of the two

polarizations as

$$P = \frac{I_{\parallel} - I_{\perp}}{I_{\parallel} + I_{\perp}} \quad .$$

The variation of the polarization of the emerging light as plotted from the data in Figs 1. and 2. is shown in Fig. 3. The discontinuity of the curve is due to the fact that only light paths above the laser threshold can be taken into account in the emerging polarization and that the threshold results in a discontinuity of the function.

This description holds, of course, only if the polarization of the laser light is independent of the possible polarization of pumping. For dye lasers excited by polarized light, this is seldom the case.

It is apparent from Figs 1. and 2. that light paths can be singled out or suppressed at will by changing the pumping rate in spite of the spatial distribution of pumping which is assumed to be homogeneous.

The above calcualtion can readily be generalized to any spatial distribution of gain or pumping, only the integral over the given chord of the position dependent gain coefficient has to be substituted in the exponent of e in expression (3). This offers an additional possibility of singling out light paths as will be seen later in more detail when considering the modification of pumping by Gaussian excitation or by use of annular diaphragms.

The considerations of light paths mentioned above, with special regard to the properties of the emerging light, can generally be applied to superradiance and to stimulated spontaneous radiation from a circular planar laser material. The presence of reflecting surfaces does not necessarily lead to laser operation. Such surfaces have to act as a Fabry-Perot resonator, that is, to satisfy the conditions under which standing waves can be obtained. One of the possible cases is the self-locking of light paths similarly to the case of ring-lasers. Standing waves can be obtained in the case of self-locked polygons. As in the case of one-dimensional lasers the ratio of the locked light path to the wavelength of light is in most cases of the order that the condition of standing waves is satisfied within the bandwidth of the gain curve of the laser material. The results of Figs 1. and 2. can be used even in the case of discrete values which can be calculated for the self-locked polygons.

The operation of the case of polygons will be discussed without loss of generality when discussing another type of "Fresnel reflexion halo lasers" in Section IV.

III. GAUSSIAN DISTRIBUTION OF THE GAIN

The foregoing considerations concerned the conditions of higher than threshold laser operation assuming various light paths and homogeneous spatial distribution of the gain pg_o per unit length.

In practice it is usually difficult to achieve homogeneous spatial gain distribution over the plane. Let us now consider the case in which the spa-

tial distribution of the excitation is Gaussian-like and of circular symmetry resulting in a gain distribution which, owing to the gain per unit length within the laser, is of a similar Gaussian type and of circular symmetry.

Viewed from above, the centre of the circular active material is the origin of the cartesian coordinates x, y (Figure 4).

For parameter σ the intensity distribution takes in the plane the form

$$I(x,y) \sim e^{-(x^2+y^2)/\sigma^2} \quad . \tag{5}$$

The corresponding threshold gain distribution $g_o(r)$ should satisfy the relation

$$\rho(0)\exp[4\int_0^R g_o(r)dr] = 1 \quad , \tag{6}$$

where

$$g_o(r) = g_o N e^{-r^2/\sigma^2} \tag{6a}$$

and r is a distance along a diameter of the circle with radius R measured from the centre of the disc. From the threshold condition given in eq.(6) one can easily verify that the normalization factor N has to be taken in the following form:

$$N = \frac{2}{\sqrt{\pi}} \frac{(R/\sigma)}{\mathrm{erf}(R/\sigma)} \tag{6b}$$

(erf denotes the error function).

If a light path starts at angle α from the point x = (-R,0) on a chord of the circle with radius R, then ξ is the distance of a point from the point x = (-R,0),

$$0 \leq \xi \leq 2R\cos\alpha \quad . \tag{7a}$$

Using now the substitution

$$x = \xi\cos\alpha - R \quad , \qquad y = \xi\sin\alpha \quad , \tag{7b}$$

we can make use of the coordinates ξ, α, where in the original system along a straight line:

$$y = (x+R)\,\mathrm{tg}\alpha \tag{7c}$$

the gain per unit length is

$$G_\alpha(\xi) = pg_o N e^{-\frac{R^2\sin^2\alpha}{\sigma^2} - \frac{(\xi - R\cos\alpha)^2}{\sigma^2}} \quad . \tag{8}$$

Now, eq.(3) for the emerging relative intensity of the light is obtained as

$$I_k(\alpha) = I_o\rho(\alpha)^{k-1}(1-\rho(\alpha))\exp[k\int G_\alpha(\xi)d\xi] \quad , \tag{9}$$

where the total gain along a chord has the form

$$\int G_\alpha(\xi)d\xi = pg_oNe^{-\frac{R^2\sin^2\alpha}{\sigma^2}} \int_o^{2R\cos\alpha} \exp\left[\frac{(\xi-R\cos\alpha)^2}{\sigma^2}\right]d\xi \quad . \tag{10}$$

Using the substitution $\zeta = (\xi - R\cos\alpha)/\sigma$ it can readily be seen that the integral is the well-known error function. We get

$$\int G_\alpha(\xi)d\xi = pg_oN\sigma\sqrt{\pi}e^{-(R/\sigma)^2\sin^2\alpha}\operatorname{erf}(R\cos\alpha/\sigma) \quad . \tag{11}$$

Substituting this expression into eq.(9), the relative intensity of the emerging light we wish to evaluate is given as

$$I_k(\alpha) = I_o\rho(\alpha)^{k-1}(1-\rho(\alpha))\exp\left[\frac{2kpg_oR}{\operatorname{erf}(R/\sigma)}e^{-(R/\sigma)^2\sin^2\alpha}\operatorname{erf}(R\cos\alpha/\sigma)\right] \quad . \tag{12}$$

Numerical calculations have been made by use of this equation for various values of the parameter σ, taking R=1, p=1 and $g_o=\frac{\ln 25}{4}$. The results are shown in Figs. 5, 6, 7.

Figure 5. clearly shows that upon concentration of the gain in the centre of the cuvette (σ is small), the light path along the diagonal becomes prominent and that this path is the only one along which the laser works when the gain is close to the threshold.

Figure 6. shows the transition due to the increase in σ. The prominence of the diagonal decreases and modes propagating at angles close to that of total reflexion show a gradual increase. For $\sigma \geq 0.5$ (Figure 7) the curve is practically the same as that reproduced in Figure 1. and 2. for homogeneous excitation.

It can be inferred from the above that down to $\frac{\sigma}{R} > 0.5$ the homogeneous gain distribution postulated in the foregoing as well as in the subsequent considerations permits the processes taking place in halo lasers to be reasonably well described. For $\frac{\sigma}{R} \leq 0.1$, only modes propagating around the diagonal are available for operation, thus they can be well isolated from other modes if the excitation is comparable to Gaussian distribution.

Results of the here described method of calculation will appreciably deviate from those discussed above (homogeneous excitation) only if $\frac{\sigma}{R} < 0.5$.

IV. DOUBLE-WALLED HALO LASERS

A special group of planar lasers consists of disc-shaped active material surrounded by two other materials with unlike refraction indices. A typical case of such an arrangement is the dye laser excited through the bottom plate of an adjustable cylindrical cuvette as described in the reported experiments [2] - [4]. A similarly typical case could be, for example, a disc-shaped active solid with a concentric resonator separated from the active material by air. Expressions used in the numerical calculations concerning dye lasers, taken as an example, should hold in other similar cases, too.

The thickness of the active material normal to the plane of excitation is still taken to be negligible, that is, the divergence normal to the laser plane is not being considered here. However, the light paths covered by "whispering" or "shouting" modes in the passive glass wall are now taken into account.

As a general case, the schematic drawing in Figure 8. is referred to. Here the active material with radius R and of refraction index n_1 is surrounded by a cylinder of wall thickness d having a refraction index n_2; outside the cylinder the refraction index is n_o. Reflexions from the interface n_1-n_2 can be neglected since the here generated modes correspond with the substitution $n_o \equiv n_2$ to cases which have been already discussed (Section II). Moreover, it is apparent from Figure 8. that at angles of incidence generating modes capable of emergence the reflexions from this surface are not more than 1% which even in the case of normal incidence is only a quarter of the reflexions from the n_2-n_o interface considered here.

In the calculation to follow, the possible ring laser modes (including those around the diagonal) will be considered when the light emerging from paths corresponding to closed polygons has to be evaluated. On substituting the actual value of the number of reflexions k, and putting $n=n_1$, $n_2=n_o=1$, these calculations will yield the corresponding data for simple disc-shaped halo laser made of a single material as discussed previously.

The definitions are given without loss of generality for an equilateral triangle.

a) Calculation of light paths

The polygon we are trying to find is determined by the interior central angle 2γ made by the two lines drawn from two of its adjacent vertices to the n_o-n_2 interface (for a triangle $\gamma=60^o$). Half the vertex angle formed on the n_o-n_2 surface is α. The refraction angles of the n_1-n_2 interface are Θ and β. The light path along a side of a polygon in the active material is 2a; that in the passive material of refraction index n_2 (e.g. glass) is 2b along the same side of the polygon.

Correspondingly, if the polygon has k sides, (k-1) reflexions are received on the n_o-n_2 surface and the length of the light path is 2ka in the active, and 2kb in the passive material. Calculating with the condition of standing

waves, the sum of path lengths has to be modified with respect to each refraction index in order to get correct values of the free spectral range (FSR) for different closed polygons (see Section VII).

If the values of n_o, n_1, n_2 and γ are given according to the symbols used in Fig. 8., it is possible to calculate numerically a, b and α to any accuracy by solving simultaneously equations

$$\frac{\sin\Theta}{\sin\beta} = \frac{n_2}{n_1}$$

$$\cos\beta = [R^2 + b^2 - (R + d)^2]/2Rb$$

$$b^2 = R^2 + (R + d)^2 - 2R(R + d)\cos\alpha \qquad (13)$$

$$\alpha = \gamma + \Theta - \pi/2$$

Since analytical formulae for a, b and α are extremely complicated, it was thought to be more convenient to plot from the data obtained by numerical calculations their variation as a function of $\frac{d}{R}$ for some typical cases (Figs. 9, 10). Figure 11. shows the dependence of the parameters on the relative refraction index for $\frac{d}{R} = 0.4$ in the case of a triangle. In this figure also the limit angle η for total reflexion is to be seen, this angle constitutes a limit between the imprisoned "whispering" and the "shouting" modes capable of emergence and it plays an important role in the selection of the number of emerging modes.

b) Amplification

To evaluate the gain, it is again the Fresnel reflections which are taken into account. The relative intensity of the light is again given by use of (3) taking k reflexions and a light path of length 2ka in the active material as

$$I_{\parallel,\perp}/I_o = \rho_{\parallel,\perp}(\alpha)^{k-1}(1 - \rho_{\parallel,\perp}(\alpha))\exp(2akpg_o) \qquad (14)$$

This expression holds for any polygon with k interior angles. The definition of g_o is given by (4), α can be evaluated from (13).

Numerical values of $I_{\parallel,\perp}$ for some typical light paths are plotted in Figure 12. as a function of p with cuvette parameter $\frac{d}{R} = 0.4$. Relative intensities around the threshold gain as a function of p are shown for modes separated from one another in the polarization. The solid lines represent intensities of modes capable of emerging and of an activity above the threshold within the laser; modes in the region given by the broken lines still have intensities below the threshold of laser operation. The figure clearly shows that modes can be selected by modifying the pumping even if the spatial distribu-

tion of the gain is homogeneous. For instance, the diagonal is the only useful component in the range $1 \leq p \leq 1.4$; as the gain increases the perpendicular component of the triangle enters the scene and so on. For a given pumping, the weight of each mode can be estimated from the value of I of the light emerging for the corresponding p.

An interesting phenomenon observable in the figure is the appearance of 5- and 7-pronged stars which can be extrapolated to higher order star-shaped modes. The slope of the curve increases as the number of prongs increases but the threshold of operation shifts to ever higher gains. If the excitation is very intense the star-shaped modes would probably dominante; however, in the usually observed range of the operational threshold of lasers their occurence is not to be expected.

The figure shows another noteworthy phenomenon, viz. the hexagonal mode of perpendicular polarization which exhibits a gain exceeding the threshold of laser operation within the cuvette, however, only small fraction of the light can leave the cuvette because of the high value of the reflexion.

As originally assumed, then experimentally verified, the here described modes may lay in any direction within the operational plane of the laser, consequently the modes can occupy all possible positions in the cuvette. For this reason the relative intensities evaluated as above can be checked only if the modes are separated from one another during detection as to be described in Section VIII.

If the total intensity is measured by observing the halo laser from a given point on the operational plane of the laser when the emitted light is averaged over the total solid angle of the cuvette viewed from the detector, the modes which are not associated with the diagonal have to be calculated with double weight if a circular run in two directions, similar to that observed in ring lasers, is not prevented.

In the above calculations the gain was assumed to be homogeneously distributed in space. The conditions are not essentially different for Gaussian excitation since, as it was shown in Section III (see Figure 7.) Gaussian distributions with parameter $\frac{\sigma}{R} > 0.5$ can practically be considered homogeneous. Values for $\frac{\sigma}{R} < 0.1$ are close to those obtained for special annular excitation where $e = 0$ and $\Delta e = \frac{\sigma}{R}$ (see Section V).

V. HOMOGENEOUS ANNULAR PUMPING

Modes in halo lasers are most conveniently identified by their light paths running along polygons in order to satisfy the condition of the production of standing waves. The most important and at the same time the simplest polygons show most of the gain in an annular region concentric with the centre of the halo laser.

A given mode shows no gain in the inscribed circle of the polygon and its light path is short close to the cylindrical wall, in the region populated

by whispering modes incapable of emergence. If a laser material is chosen by which no considerable light is being absorbed in the region of non-inversion, a halo laser can be excited in only one of the concentric annular bands.

The specific gain of each mode substantially increases in a given annular band whose position and thickness differ from mode to mode. This implies that a suitable choice of the pumping annular geometry permits a mode to be singled out.

Assuming annular excitation with a given geometry, the intensity of the light emerging from the path at angle α to the diagonal with a single reflexion can be evaluated by use of the same reasoning as in Section II.

If the angle of reflexion of the polygon we wish to isolate is known, the optimum geometry can be chosen either by deductive calculations (13) or from the graphs in Figs. 9, 10.

Restricting the calculation to homogeneous excitation and gain, we can show that inside the annular region of Figure 13. the gain per unit length is pg_o and that outside of this band it is zero. Reflexion and transmission are calculated as in the foregoing.

According to Figure 13, the excitation is zero up to a distance e from the centre, pg_o in the band Δe and zero again outside of this band.

We can now use expression (3) for a light path in the active region with the substitution

$$2R\cos\alpha \rightarrow 2R[((e + \Delta e)^2 - \sin^2\alpha)^{1/2} - (e^2 - \sin^2\alpha)^{1/2}]. \qquad (15)$$

Results of numerical calculations are given in Figure 14. for some cases whose conditions are specified in the figure. It is easily apparent that for $e = 0.4$ with $\Delta e = 0.1$, the mode associated with $\alpha = 25^o$, where as for $e = 0.2$ with $\Delta e = 0.1$ that with $\alpha = 12^o$ can be singled out.

VI. DIVERGENCE NORMAL TO THE PLANE

The halo laser material taken to have the form of an infinitely narrow disc does not yield any information on the divergence normal to the operational plane.

To estimate this divergence a very simplified approach will be used. Without attempting accurate calculations only those divergences will be considered which are expected to occur in two but not in one-dimensional laser devices.

Let us consider a halo laser in a double-walled case (glass cuvette), excited from below according to the reported experimental conditions [1]-[4]. The excitation and thus the gain are both homogeneous in the laser plane. However, in the direction normal to this plane the gain exponentially decreases due to the absorption of the exciting light. This fact is mainly responsible for one of the most important deviations from the behaviour of

one-dimensional lasers. As has already been shown, the appearance and intensity of each of the different modes depends, in the two-dimensional case, on the actual (here local) value of the gain. Consequently, modes are discriminated from one another upwards from the bottom plate of the cuvette in a direction normal to the operational plane, thus the "thickness" of each mode can be differentiated in the plane as well as the divergence which varies from mode to mode.

Another reason for the difference in the divergence of modes is the significant dissimilarity of length of light paths covered by modes in the partly closed Fabry-Perot resonator.

A further contribution to the divergence is due to the fact that in Fresnel reflexion halo lasers the threshold pumping rate for different polarizations differs because each mode is reflected at another angle resulting in a difference between the thicknesses, thus divergences of the two polarization components in identical polygons.

It follows from the above that a strongly mode dependent divergence is to be expected which, moreover, appreciably varies with polarizations.

Intensity variations of the divergence along with the asymmetry of pumping are now left out of consideration. For the present calculation all modes normal to the plane are taken to be of constant intensity and of a thickness corresponding to the length of the path from the bottom plate to that of the path associated with threshold gain.

If the absorption coefficient for the excitation is q, then for a gain pg_o at the bottom plate the gain coefficient in thickness h reckoned from the bottom plate is given as

$$g(h) = pg_o e^{-qh} \tag{16}$$

For parallel or perpendicular polarization and the corresponding reflexion coefficient, the threshold gain for initiating laser operation can be evaluated for a polygon of k sides from the equation

$$\rho_{\parallel,\perp}(\alpha)^{k-1} \exp[g(h_o)\,2ka] = 1, \tag{17}$$

which gives

$$g_{\parallel,\perp}(h_o) = -\frac{(k-1)\ln\rho_{\parallel,\perp}(\alpha)}{2ka}\,.$$

The solution to eq. (16) for this value given the "thickness" of the mode associated with the given polarization and polygon in the form

$$h_{o_{\parallel,\perp}}(k) = \frac{1}{q}\left[\ln(pg_o) - \ln\frac{(k-1)\ln\rho_{\parallel,\perp}^{-1}(\alpha)}{2ka}\right]. \tag{18}$$

The resonator length calculated in the case of one-dimensional lasers

corresponds here to the sum of the lengths of the sides of a k-gon which according to Fig. 8., is given as

$$\ell = 2k(a + b), \tag{19}$$

and it is, of course, independent of polarization.

The approximation will not be worse if the divergence (D) is expressed as

$$D \approx \frac{h_o}{\ell}, \tag{20}$$

which, on substitution of (18) and (19), takes the form

$$D_{\parallel,\perp}(\alpha) = \frac{1}{2qk(a+b)}\left[\ln pg_o - \ln \frac{(k-1)\ln\rho_{\parallel,\perp}^{-1}(\alpha)}{2ka}\right]. \tag{21}$$

Owing to the crudeness of the approximation, the usefulness of the expressions is only qualitative, nevertheless they are fairly illustrative of the particular divergences observable in halo lasers.

In agreement with experimental evidence, the results clearly show that the divergence varies with both mode and polarization, it increases with increasing pumping rate, and it can be reduced by increasing both the resonator size and the absorption coefficient of excitation (except in the case of waveguiding formation).

Similarly to all calculations made up to the present, the competition of modes, by which results can be substantially modified, has not been taken into account. Particularly, the observation of the separation of modes running along identical polygons but with different polarizations becomes impracticable since the light with polarization with the higher reflexion coefficient will be amplified at the expense of the other running along the same polygonal light path.

VII. THE FREE SPECTRAL RANGE (FSR)

The measurement of halo laser spectra yields information which permits inferences to be made on the nature of modes involved in the operation of halo lasers. One of the most important data for the identification of different modes is the spacing of spectral lines in the halo laser since each mode propagates along a specific light path and leaves the laser at a given angle.

The FSR can be evaluated from the known expression

$$\Delta\lambda_{oi} = \frac{\lambda_o^2}{2n\ell_i} \tag{22}$$

where n is the refraction index, λ_o is the wavelength of laser light in vacuum, $\Delta\lambda_o$ is the spacing of lines in the spectrum, ℓ_i is the spacing of

reflector surfaces in the actual Fabry-Perot subresonators.

For halo lasers generated in homogeneous material (e.g. solids), ℓ_i is, for example, the length of the light path along the closed polygon associated with the mode in question (see Fig. 8), that is,

$$\Delta\lambda_o = \frac{\lambda_o^2}{4n_1 kR\cos\alpha} \tag{23}$$

where k is the number of relexions for a closed polygon.

In the case of a double-walled planar laser, the double reflexion from the cuvette wall (active material - cuvette, cuvette -air) has to be introduced into (22) where the values of b from (13) have to be substituted for ℓ_i. If we have to deal with a closed polygon, the optical length of the path taken in both materials has to be substituted for the given mode in the form

$$\Delta\lambda_o = \frac{\lambda_o^2}{4k(n_1 a+n_2 b)} \tag{24}$$

where n_1 and n_2 are values of the refraction index for the active material and the cuvette wall, respectively; a and b are light paths according to Figure 8.

In practice, modes can be identified from the measured FSR values. If we take into account the numerical values of reflexions the modulation depth can also be determined.

VIII. MODE SEPARATION OF HALO LASER

It has been shown that different planar laser modes emerge at different angles from halo laser sources. This permits the light of a mode emerging in a given planar direction to be isolated and observed without interference from other modes.

A possible way to do this is to inspect the modes through a slit not too far from and lying normal to the operational plane of the laser, then to select a mode in the plane normal to the straight line connecting the centre of the halo laser to the slit.

The arrangement and the symbolization are given in Figure 15. Observed modes are identified by the central angle of the polygon associated with the mode. Rays of light emerging from modes are tangents of the inscribed circle of the polygon associated with any given mode. In the plane of measurement the mode is determined (neglecting the refraction index) by the tangent drawn from the centre of the slit to the internal circle of the polygon. The distance from the centre shown in the figure can be evaluated in the plane of measurement from simple geometrical considerations, as

$$f(\gamma) = R\,\frac{L-m}{(m^2-R^2\cos^2\gamma)^{1/2}}\,\cos\gamma \tag{25}$$

If the relative refraction index of the active material is n, then the mode associated with the polygon can be selected for the known central angle by solving successively the set of equations

$$\varkappa = \arcsin[n \sin(\frac{\pi}{2} - \gamma)]$$

$$\omega = \arcsin[\frac{R}{m} \sin(\pi-\varkappa)] \qquad (26)$$

$$f(\gamma) = (L-m)\,\mathrm{tg}\omega$$

IX. CONCLUSION

Radiation emitted from two-dimensional disc-shaped laser material has been reviewed for the light emerging because of Fresnel reflexions in the partly closed cylindrical Fabry-Perot resonator constituting the natural surrounding of the material. The calculations presented show that a proper choice of pumping, which permits the value and the spatial distribution of the gain to be conveniently set, enabled a planar laser of a single mode to be obtained. The results prove at the same time that a substantial suppression of modes from a laser active material can be achieved even without the use of one-dimensional open Fabry-Perot resonator. Estimations have been given on the experimentally verifiable parameters of divergence, FSR and of the experimental separation of modes. A number of simplifying approximations used in the calculations do not essentially effect the particularities of the phenomena in question. It was found that the dependence of intensity of the reflected light on the angle of incidence and on the polarization as well as the fact that the lengths of the light paths in the two-dimensional resonator appreciably differ from mode to mode and that they dominate at different points of the active material, are properties which are not usually encountered in one-dimensional lasers. It is thought that more accurate investigations may lead to the prediction of new laser physical phenomena, to their experimental verification and, where useful, to their practical application.

ACKNOWLEDGEMENT

The authors would like to thank Dr. Gy. Farkas and Dr. M. Jánossy for encouragement and stimulating discussions.

REFERENCES

[1] Z.Gy. Horváth, A.A. Malyutin and A.V. Kilpio, "Halo" Laser Device", Preprint KFKI-1979-17 (1979)

[2] Zs. Bor, B. Rácz, G. Szabó and Z.Gy. Horváth, "Two-Dimensional Halo Laser Performance", Phys. Lett. 80A 153 1980 ; 11. IQEC, Boston, R20, (1980); JOSA 70 1410 (1980)

[3] Z.Gy. Horváth, A.V. Kilpio, A.A. Malyutin and Yu.N. Serdyuchenko, "Picosecond Two-Dimensional "HALO" Superradiance and Laser in Rhodamin 6G," Optics Comm. 35 142 (1980)

[4] Z.Gy. Horváth, "Light Time-of-Flight Method for Topological Investigation of a Two-Dimensional "Halo" Laser Performance", Proc. of the 9th Symposium of the IMEKO TC on Photon Detectors p. 240, Visegrad, Hungary Sept. 9-11 (1980)

[5] F.H. Nicoll, "Far-Field Pattern of Electron-Bombarded Semiconductor Lasers" Proc. IEEE 55 114 (1967)

[6] S. Wang and S. Sheem, "Two-Dimensional Distributed-Feedback lasers and their Applications" Appl. Phys. Lett. 22 460 (1973)

[7] M. Yamanishi, I. Suemune, M. Kohno, N. Mikoshiba and T. Kawano, "Oscillation of Two-Dimensional Modes in Transverse-Distributed-Feedback Cavity Lasers" Jap. J. Appl. Phys. 19 L739 (1980)

[8] W.H. Kegel, "Natural Masers", Appl. Phys. 9 1 (1976)

[9] A. Hardy and D. Treves, "Amplified Spontaneous Emission in Spherical and Disk-Shaped Laser Media", IEEE J. Quantum El. EQ-15 887 (1979)

[10] J.A. Glaze, S. Guch and J.B. Trenholme, "Parasitic Suppression in Large Aperture Nd: Glass Disk Laser Amplifiers", Appl. Optics 13 2808 (1974)

[11] G.P. Kostometov and N.N. Rozanov, "Amplified Spontaneous Radiation Emitted from Disk Laser Amplifiers", Sov. J. Quantum El. 6 696 (1976)

[12] A.L. Schawlow and C.H. Townes, "Infrared and Optical Masers" Phys. Rev. 112 1940 (1958)

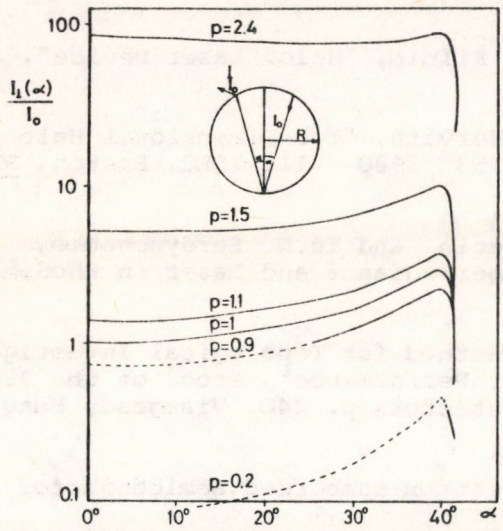

R=1
n=0.66 (n_i=1.51, n_o=1)
k=2
g_o=0.8

Fig. 1.

Angular dependence of the outcoming normalised intensity $I_\perp(\alpha)/I_0$ after two reflexions in the case of perpendicular polarisation at different values of pumping parameter p. Dashed lines refere to pumping below threshold.

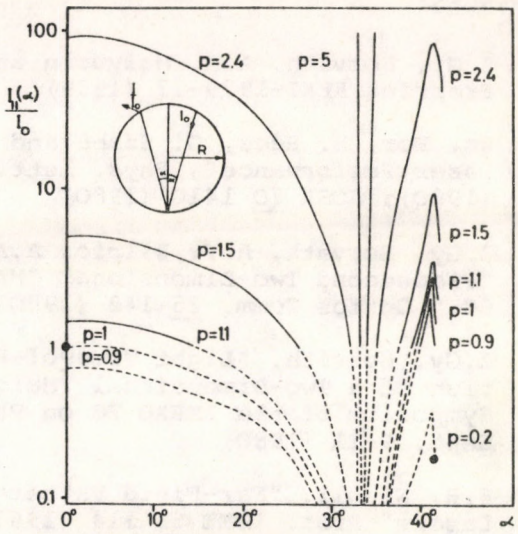

R=1;
n=0.66 (n_i=1.51, n_o=1);
k=2;
g_o=0.8

Fig. 2.

Angular dependence of the outcoming normalised intensity $I_\parallel(\alpha)/I_0$ after two reflexions in the case of parallel polarisation at different values of pumping parameter p. Dashed lines refer to pumping below threshold.

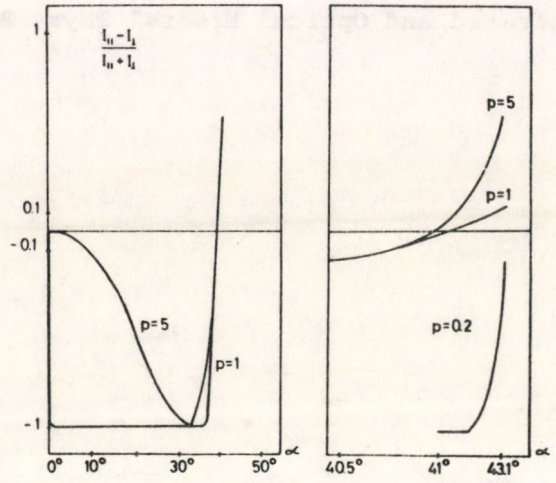

Fig. 3.

Angular dependence of the degree of polarisation $P=(I_\parallel-I_\perp)/(I_\parallel+I_\perp)$ of the emerging light calculated from the data in Figs. 1. and 2.

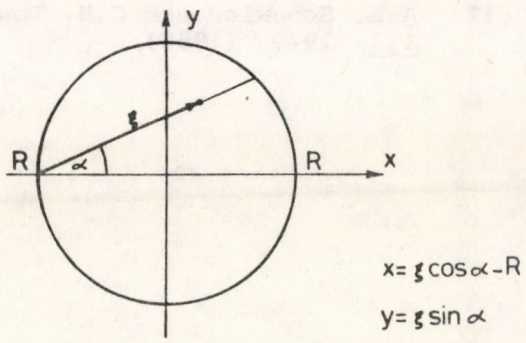

Fig. 4.

Variables used in the text in the description of halo laser action in the case of Gaussian spatial distribution of excitation.

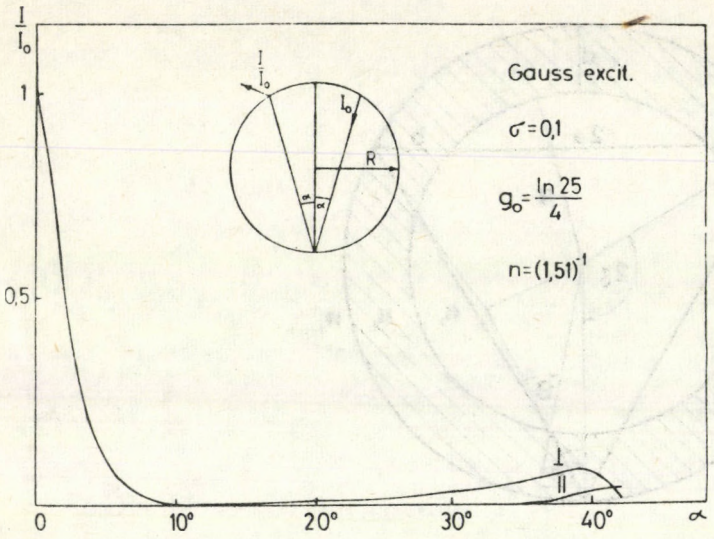

Fig. 5.

Angular dependence of the emerging relative intensity in the case of a narrow (σ=0.1) Gaussian spatial distribution of excitation.

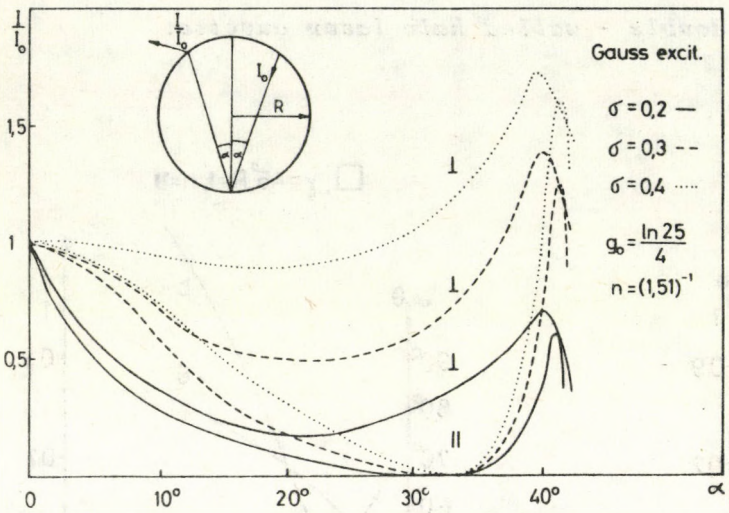

Fig. 6.

Angular dependence of the emerging relative intensities in the case of Gaussian spatial distributions of excitation for σ=0.2, 0.3 and 0.4.

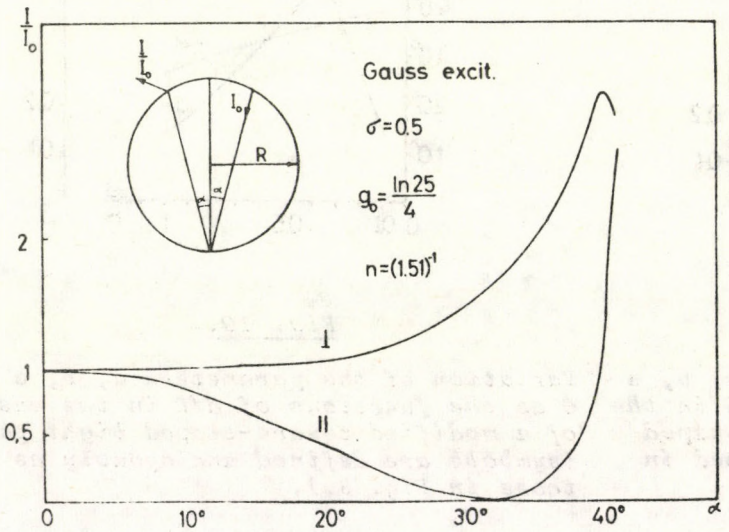

Fig. 7.

Variation of the intensity function $I(\alpha)/I_0$ in the case of a broad σ=0.5 Gaussian spatial distribution of excitation.

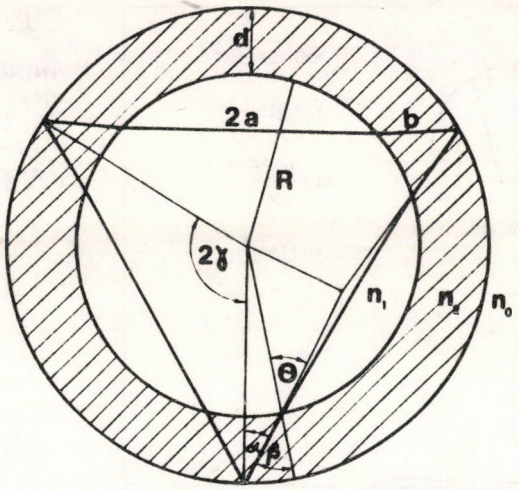

Fig. 8.

Cross section of a double - walled halo laser cuvette.

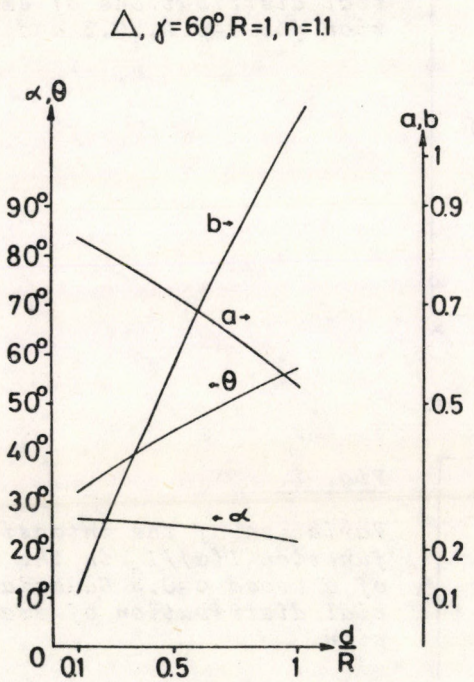

Fig. 9.

Variation of the parameters a, b, α and Θ as the functions of d/R in the case of a modified triangle-shaped light path (symbols are defined in Fig. 8.)

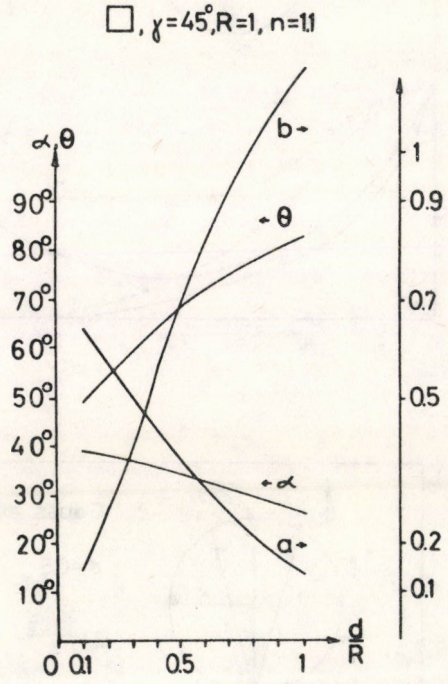

Fig. 10.

Variation of the parameters a, b, α and Θ as the functions of d/R in the case of a modified square-shaped light path (symbols are defined analogously as those in Fig. 8.).

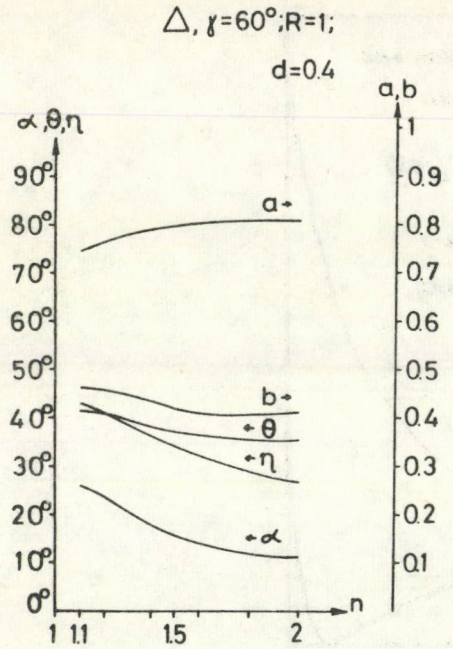

Fig. 11.

The dependence of the parameters a, b, α, θ and η (limit angle for total reflection) on the relative refraction index for d/R=0.4 in the case of a modified triangle.

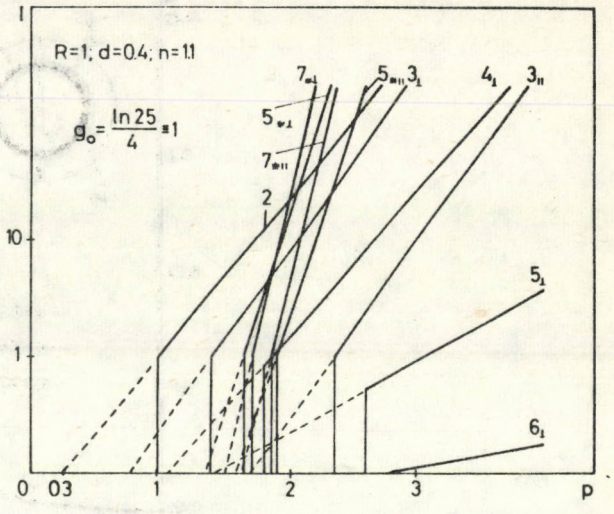

Fig. 12.

Numerical values of the outcoming relative intensities I/I_0 as the functions of pumping parameter p. Notations 3, 4, etc. refer to 3, 4, etc. angle konvex polygons, and 5 and 7* refer to 5 - and 7 - pronged stars, respectively.*

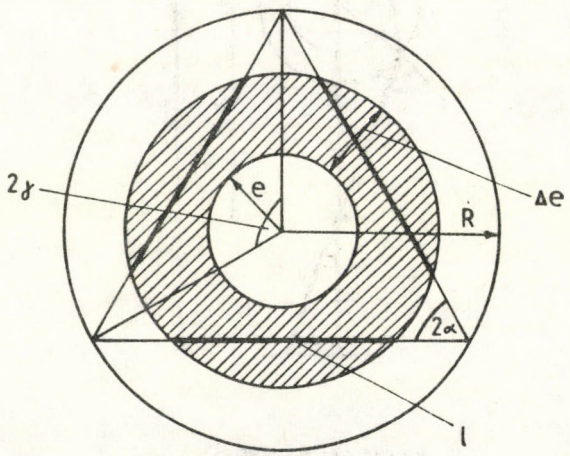

Fig. 13.

Schematic drawing of the cross section of a halo laser in the case of annular excitation. The excited region of the plane is shaded.

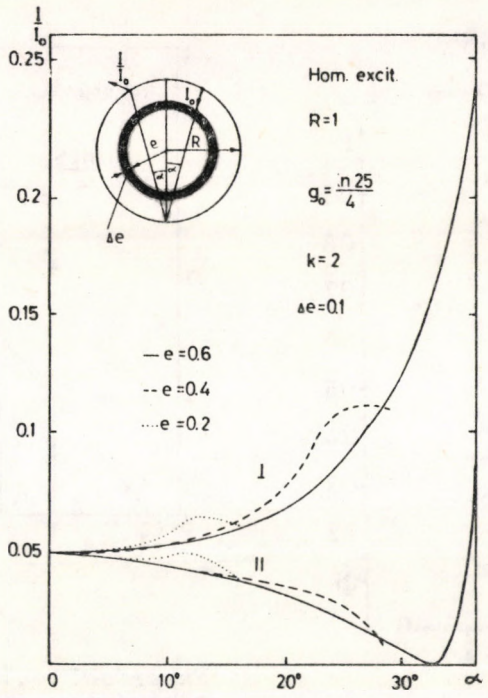

Fig. 14.

Angular dependence of the emerging relative intensity in the case of a homogeneous annular excitation.

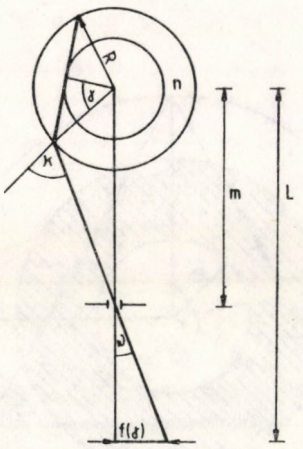

$$\varkappa = \arcsin\, n \sin(90-\delta)$$

$$\omega = \arcsin \frac{R}{m} \sin(180-\varkappa)$$

$$f(\delta) = (L-m)\,\mathrm{tg}\,\omega$$

Fig. 15.

One possible arrangement for preparation of one mode from a multimode halo laser.

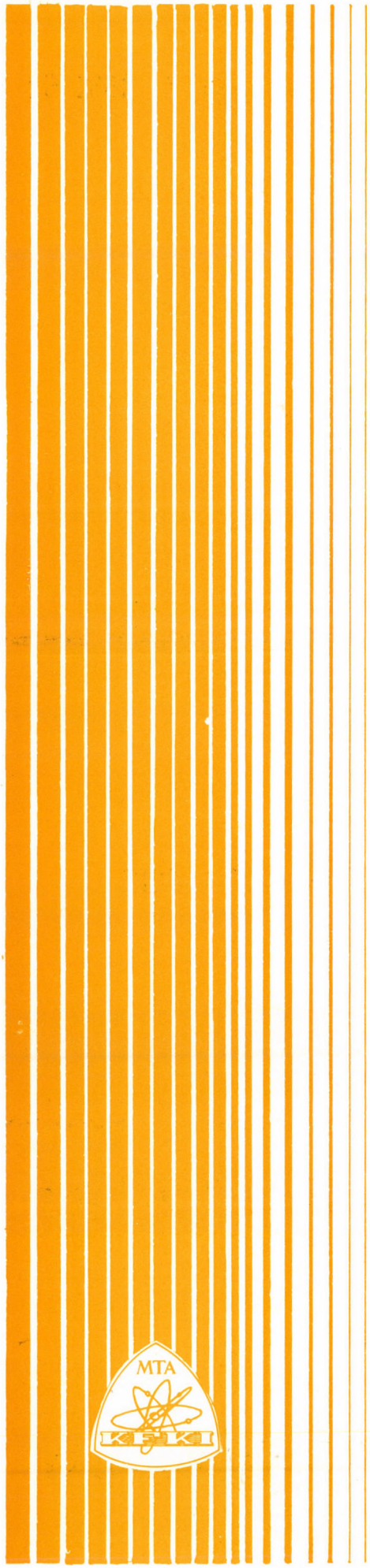

Kiadja a Központi Fizikai Kutató Intézet
Felelős kiadó: Kroó Norbert
Szakmai lektor: Jánossy Mihály
Nyelvi lektor: Harvey Shenker
Gépelte: Balczer Györgyné
Példányszám: 570 Törzsszám: 81-463
Készült a KFKI sokszorosító üzemében
Felelős vezető: Nagy Károly
Budapest, 1981. augusztus hó